J|A|C|S
ARTICLES
Published on Web 01/28/2004

Dynamics of Proton Transfer in Bacteriorhodopsin

Yong-Sok Lee*

Contribution from the Center for Molecular Modeling, Center for Information Technology, National Institutes of Health, Bethesda, Maryland 20892

Morris Krauss

Center for Advanced Research in Biotechnology, National Institute of Standards and Technology, Rockville, Maryland 20850

Received May 13, 2003; E-mail: leeys@mail.nih.gov

Abstract: Proton transfer in bacteriorhodopsin from the cytoplasm to the extracellular side is initiated from protonated asp96 in the cytoplasmic region toward the deprotonated Schiff base. This occurs in the transition from the photocycle late M state to the N state. To investigate this proton-transfer process, a quantum mechanics/molecular mechanics (QM/MM) model is constructed from the bacteriorhodopsin E204Q mutant crystal structure. Three residues, asp96, asp85, and thr89, as well as most of the retinal chromophore and the Schiff base link of lys216 are treated quantum mechanically and connected to the remaining classical protein through linker atom hydrogens. Structural transformation in the M state results in the formation of a water channel between the Schiff base and asp96. Since a part of this channel is lined with hydrophobic residues, there has been a question on the mechanism of proton transfer in a hydrophobic channel. Ab initio dynamics using the CHARMM/GAMESS methodology is used to simulate the transfer of the proton through a partially hydrophobic channel. Once sufficient water molecules are added to the channel to allow the formation of a single chain of waters from asp96 to the Schiff base, the transfer occurs as a fast (less than a picosecond) concerted event irrespective of the protonation state of asp85. Dynamic transfer of the proton from asp96 to the nearest water initiates the organization of a strongly bonded water chain conducive to the transfer of the proton to the Schiff base nitrogen.

1. Introduction

Photoabsorption by retinal bound in the membrane protein, bacteriorhodopsin, drives a proton through the protein and across the membrane.[1] The photocycle has been characterized spectroscopically into a series of intermediates that ultimately return to the ground state. The structural basis of the proton transport mechanism has been determined in a wide range of crystal structures of the ground and intermediate states in the photocycle.[1−5] Mutation studies have identified critical residues at different points in the cycle.[6,7] Proton transfer from the cytoplasm to the extracellular side is initiated from protonated asp96 in the cytoplasmic region toward the deprotonated Schiff base. The deprotonated Schiff base has a large effective proton affinity because of interaction with an overall H-bonding complex containing asp85, asp212, and thr89 that stabilizes the protonated Schiff base. Asp96 and the Schiff base are buried well within the protein and communicate with each other in the course of the photocycle.

In the early stage of the cycle, the protonated Schiff base is directed away from asp96 by a H-bonded network of waters and asp85 and asp212. In an M state described by the crystal structure, 1F4Z,[8] of the E204Q mutant,[1] these groups are now facing each other in position for the proton from asp96 to transfer to the deprotonated Schiff base through a narrow channel between them. A number of crystal structures as an initial model could be used that allow the Schiff base cytoplasmic accessibility.[9] The crystal structures show movement in the F and G helices. This results in the channel between asp96 and the Schiff base N that is observed in the E204Q structure. The helical movements are large enough for water to enter the channel.[10,11] The E204Q structure shows the water binding in the channel to polar residues but not in the hydrophobic region. Because of a hydrophobic patch in part of the channel, there has been concern on how the water chain required for the proton transport can form.[1,12] However, single chain water transport has been demonstrated through hydrophobic carbon nano-

(1) Luecke, H.; Schobert, B.; Cartailler, J. P.; Richter, H. T.; Rosengarth, A.; Needleman, R.; Lanyi, J. K. *J. Mol. Biol.* **2000**, *300*, 1237−55.
(2) Kamikubo, H.; Oka, T.; Imamoto, Y.; Tokunaga, F.; Lanyi, J. K.; Kataoka, M. *Biochemistry* **1997**, *36*, 12282−7.
(3) Sass, H. J.; Buldt, G.; Gessenich, R.; Hehn, D.; Neff, D.; Schlesinger, R.; Berendzen, J.; Ormos, P. *Nature* **2000**, *406*, 649−53.
(4) Rouhani, S.; Cartailler, J. P.; Facciotti, M. T.; Walian, P.; Needleman, R.; Lanyi, J. K.; Glaeser, R. M.; Luecke, H. *J. Mol. Biol.* **2001**, *313*, 615−28.
(5) Lanyi, J. K.; Schobert, B. *J. Mol. Biol.* **2002**, *321*, 727−37.
(6) Braiman, M. S.; Mogi, T.; Marti, T.; Stern, L. J.; Khorana, H. G.; Rothschild, K. J. *Biochemistry* **1988**, *27*, 8516−20.
(7) Stern, L. J.; Ahl, P. L.; Marti, T.; Mogi, T.; Dunach, M.; Berkowitz, S.; Rothschild, K. J.; Khorana, H. G. *Biochemistry* **1989**, *28*, 10035−42.
(8) Berman, H. M.; Westbrook, J.; Feng, Z.; Gilliland, G.; Bhat, T. N.; Weissig, H.; Shindyalov, I. N.; Bourne, P. E. *Nucleic Acids Res.* **2000**, *28*, 235−42.
(9) Subramaniam, S.; Henderson, R. *Biochim. Biophys. Acta* **2000**, *1460*, 157−65.
(10) Subramaniam, S.; Henderson, R. *Science* **2000**, *406*, 653−7.
(11) Radzwill, N.; Gerwert, K.; Steinhoff, H. J. *Biophys. J.* **2001**, *80*, 2856−66.
(12) Lanyi, J. K. *J. Phys. Chem. B* **2000**, *104*, 11441−8.

tubes,[13,14] suggesting that proton transport can be supported by the water chain in a hydrophobic channel. Transfer of water into a hydrophobic channel of bacteriorhodopsin has also been shown to be thermodynamically favorable.[15] There is also evidence that such a partially hydrophobic channel will support water chains required for proton transfer in cytochrome *c* oxidase.[16]

The Schiff base proton is initially removed by the asp85,[17−19] and it is generally assumed that asp85 is protonated in the M state. However, this proton may, for example, be shared within a close-coupled H-bonding network that includes thr89, asp212, two tyrosines directly bound to asp212, and the water network between these residues.[20] An extended H-bond network is required for the proton transfer.[21] Although the consensus is that asp85 is protonated in both the M and N states, a partial occupancy of the anionic state may also occur. Asp85 and asp212 are found to have comparable effective proton affinities in the M state.[22] Protonated asp212 was assigned to a 1738 cm^{-1} peak observed in the M state by a D212E mutation, showing that there is partial occupancy of the protonated state with the transfer attributed between asp212 and the hydrogen-bonded tyrosines.[6,23] Asp85 and asp212 are separated by only one water, and both are close to the Schiff base in this M state structure, 1F4Z.[1] The IR band of the side chain of thr89 is interpreted to support a direct and relatively strong H-bond to thr89[24] through the cycle from the ground state to the M state. Evidence is presented that asp85 is protonated while H-bonded to thr89.[24] However, a theoretical model of the H-bonding of asp85 to thr89 yields a very substantial shift of hundreds of cm^{-1} when changing the ionicity of asp85 (to be published elsewhere). The IR spectroscopic evidence is difficult to interpret but suggests that asp85 is anionic either transiently or through part of the M state of the cycle. Since the proton-transfer event occurs so rapidly, both charge states of asp85 must be considered.

Dynamics of proton transfer requires that ab initio quantum chemistry is required for the protein residues and the Schiff base bound retinal where strong ionic H-bonds are made and broken. There are a number of QM/MM studies of the early part of the photocycle,[25] but the proton transfer in the later photocycle has not been studied. The initial conformation for a dynamics study is obtained from a crystal structure where the essential requirements for proton transfer are met which are (i) the orientation of the Schiff base nitrogen and protonated asp96 toward each other and (ii) a single water channel possible between helices F and G. The dynamics study uses CHARMM that incorporates the GAMESS quantum chemistry package.[26,27] The rapid motion of the waters in the channel and the short time required for transfer of the proton can be studied with ab initio quantum chemistry to obtain insight into the basic features of the proton transfer between asp96 and the Schiff base. Ab initio optimization and dynamics will reorganize H-bonding patterns that are driven by strong ionic interactions in this active site. The E204Q mutant crystal structure provides a clear opening between asp96 and the Schiff base.[1] The mutation is relatively far from the proton-transfer channel and should not affect the local H-bonding pattern around asp96 or the Schiff base.

Three bonding arrangements for asp85 are considered here for the quantum model. The first considers asp85 anionic starting from the 1F4Z structure with the thr89 OH group directly H-bonded to OD1 of the carboxylate of asp85. Starting from the optimized structure obtained in the first anionic arrangement, two neutral cases were constructed by adding a proton to the carboxylate of asp85. In the second arrangement, the OH group of thr89 donates its proton to the backbone carbonyl of asp85 while the OD1H of protonated asp85 is H-bonded to the OH of thr89. In the third arrangement, the OD1H group of protonated asp85 is just H-bonded to the OH of thr89. The three cases explore the effect of the change in the state of protonation of asp85 and alternative H-bonding arrangements between asp85 and thr89 on the proton-transfer behavior. Proton transfer in relatively short times is observed for both the anionic and protonated asp85 in the second arrangement.

Methodology

Combined Potentials of Quantum Mechanics and Molecular Mechanics. An ab initio QM/MM method is required to study the dynamic proton-transfer process in bacteriorhodopsin. In the present QM/MM method,[26,27] the active-site atoms of the protein are treated quantum mechanically with the GAMESS−US[28] electronic structure code while the bulk of the protein is treated classically using the CHARMM potential.[29] Both restricted Hartree−Fock (HF) and B3LYP density functional (DFT/B3LYP) methods are available in GAMESS, allowing the dynamics to be studied at different levels of accuracy with the DFT results expected to provide the more accurate structural and energetic results.[30] An interaction potential is applied through linker atom hydrogens to properly interface the two distinct regions. This method has been successfully utilized to model the catalytic mechanism of aldose reductase[27] and chorismate mutase[31] where multiple hydrogen-bonding interactions occur between substrate and protein.

Partitioning, Energy Minimization, and Dynamics Simulations. The coordinates of the E204Q mutant of bacteriorhodopsin[1] were obtained as structure, 1F4Z, from the Protein Data Bank.[8] Lipids were removed from the X-ray structure, and hydrogens were added to the amino acid residues of bacteriorhodopsin with the HBUILD routine of CHARMM. This complex was then hydrated by placing it into a sphere of water molecules and subsequently deleting all water molecules except those with oxygens at least 2.5 Å away from the complex. After hydration, water molecules located more than 4.5 Å away from the complex were removed. A total of 167 water molecules were used for hydration.

(13) Hummer, G.; Rasaiah, J. C.; Noworyta, J. P. *Nature* **2001**, *414*, 188−90.
(14) Berezhkovskii, A.; Hummer, G. *Phys. Rev. Lett.* **2002**, *89*, 064503.
(15) Roux, B.; Nina, N.; Pomes, R.; Smith, J. C. *Biophys. J.* **1996**, *71*, 670−81.
(16) Wikstrom, M.; Verkhovsky, M. I.; Hummer, G. *Biochim. Biophys. Acta* **2003**, *1604*, 61−5.
(17) Braiman, M. S.; Bousche, O.; Rothschild, K. J. *Proc. Natl. Acad. Sci. U.S.A.* **1991**, *88*, 2388−92.
(18) Pfefferle, J. M.; Maeda, A.; Sasaki, J.; Yoshizawa, T. *Biochemistry* **1991**, *30*, 6548−56.
(19) Sasaki, J.; Lanyi, J. K.; Needleman, R.; Yoshizawa, T.; Maeda, A. *Biochemistry* **1994**, *33*, 3178−84.
(20) Needleman, R.; Chang, M.; Ni, B.; Varo, G.; Fornes, J.; White, S. H.; Lanyi, J. K. *J. Biol. Chem.* **1991**, *266*, 11478−84.
(21) Lecoutre, J.; Tittor, J.; Oesterhelt, D.; Gerwert, K. *Proc. Natl. Acad. Sci.* **1995**, *92*, 4962−6.
(22) Song, Y.; Mao, J.; Gunner, M. R. *Biochemistry* **2003**, *42*, 9875−88.
(23) Rothschild, K. J.; Braiman, M. S.; He, Y. W.; Martit, T.; Khorana, H. G. *J. Biol. Chem.* **1990**, *265*, 16985−91.
(24) Kandori, H.; Yamazaki, Y.; Shichida, Y.; Raap, J.; Lugtenburg, J.; Belenky, M.; Herzfeld, J. *Proc. Natl. Acad. Sci. U.S.A.* **2001**, *98*, 1571−6.
(25) Hayashi, S.; Tajkhorshid, E.; Schulten, K. *Biophys. J.* **2002**, *83*, 1281−97.
(26) Eurenius, K. P.; Chatfield, D. C.; Brooks, B. R.; Hodoscek, M. *Int. J. Quantum Chem.* **1996**, *60*, 1189−1200.
(27) Lee, Y. S.; Hodoscek, M.; Brooks, B. R.; Kador, P. F. *Biophys. Chem.* **1998**, *70*, 203−16.
(28) Schmidt, M. W.; Baldridge, K. K.; Boatz, J. A.; Elbert, S. T.; Gordon, M. S.; Jensen, J. H.; Koseki, S.; Matsunaga, N.; Nguyen, K. A.; Su, S. J.; Windus, T. L.; Dupuis, M.; Montgomery, J. A. *J. Comput.Chem.* **1993**, *4*, 1347−63.
(29) Brooks, B. R.; Bruccoleri, R. E.; Olafson, B. D.; States, D. J.; Swaminathan, S.; Karplus, M. *J. Comput.Chem.* **1983**, *4*, 187−217.
(30) Sobolewski, A. L.; Domcke, W. *J. Phys. Chem. A* **2002**, *106*, 4158−67.
(31) Lee, Y. S.; Worthington, S. E.; Krauss, M.; Brooks, B. R. *J. Phys. Chem. B* **2002**, *106*, 12059−65.

Scheme 1

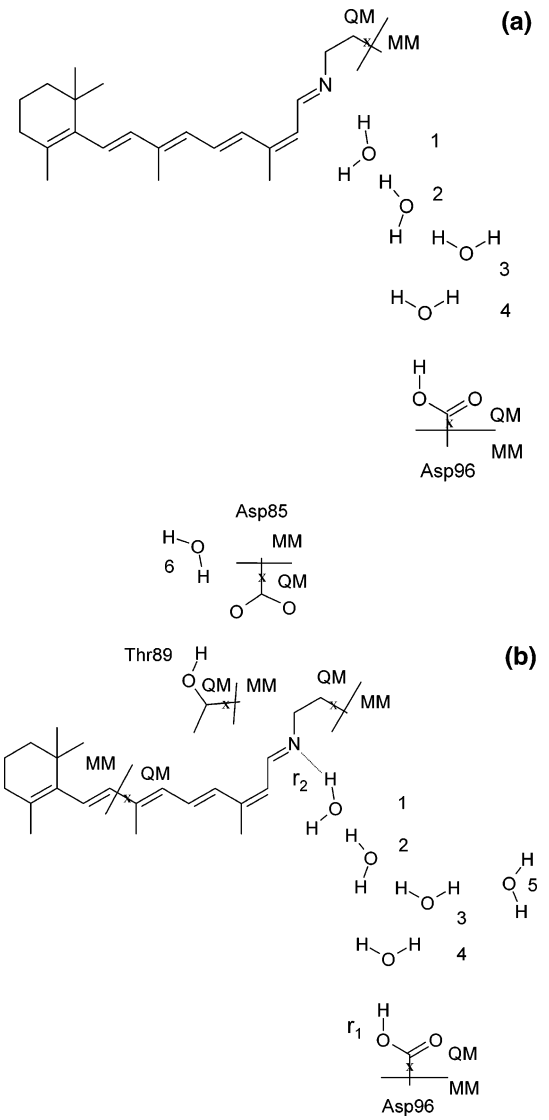

The partition of QM/MM of the Schiff base region in bacteriorhodopsin was done in two ways as depicted in Scheme 1a and 1b for the anionic asp85 case. In Scheme 1a, two water molecules labeled as 1 and 2 were inserted between the Schiff base nitrogen and the third crystal water molecule. This represents the minimal set of residues and water required for the proton transfer. Water 3 was later protonated by moving a proton from asp96 to initiate the proton transport process. This was done to determine which direction the proton would move. The QM region includes four water molecules, the carboxylate of asp96, and the retinal coupled by the Schiff base to lys216. All the atoms outside the QM region were assigned to the MM region. Each of the QM portions was connected to MM region through a hydrogen link atom as denoted by the diagonal line through the bond in Scheme 1a. After partitioning the Schiff base region, the hydrated bacteriorhodopsin was energy minimized for 200 steps with the adapted basis Newton Raphson (ABNR) method by GAMESS/CHARMM while treating the quantum atoms at the HF level with the 4-31G basis set. The energy minimization by CHARMM with an all-atom parameter set[32] was carried out with a constant dielectric constant ($\epsilon = 1$). Electrostatic force was treated with the force switch method[33] and a switching range of 8−12 Å for MM interactions and without cutoffs for QM/MM

(32) Simulation, M. *Parameter file for CHARMm*, version 22; Waltham: MA, 1992.
(33) Steinbach, P. J.; Brooks, B. R. *J. Comput.Chem.* **1994**, *15*, 667−83.

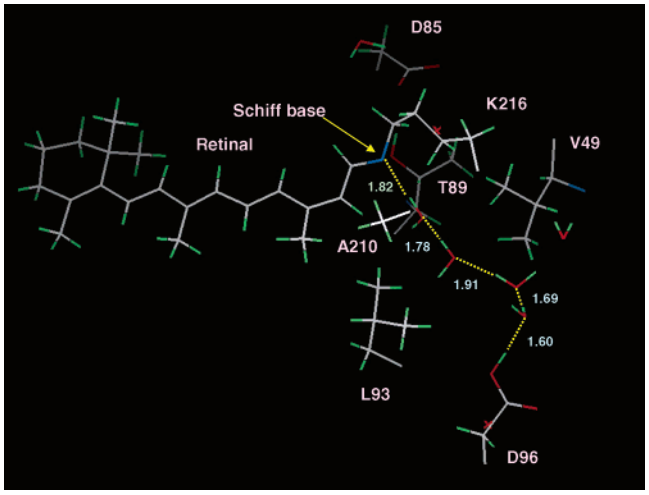

Figure 1. Snapshot at the end of 4ps QM/MM dynamics simulations while treating quantum mechanical atoms at the level of HF/4-31G. Dotted lines in yellow indicate the H-bonding interactions. Link atom hydrogen is denoted × in red. Atoms represented by colors: white, carbon; green, hydrogen; blue, nitrogen; and red, oxygen.

electrostatic interactions. van der Waals interactions were calculated with the shift method with a cutoff of 12 Å. Using the energy minimized structure as the starting point, the hydrated bacteriorhodopsin was heated to 375 K, equilibrated for 2 ps, and run for another 2 ps. Dynamics were run using Verlet integration with a time step of 1 fs. The initial velocities were assigned from a Maxwell−Bolzmann distribution at a temperature of 375 K.

The minimal model was then expanded by adding to the QM region, asp85, thr89, and two additional crystal water molecules, 5 and 6, that are H-bonded, respectively, to water 3 and to asp85. In this larger model, described in Scheme 1b, the proton transfer is attempted for both asp85 anionic and protonated. The initial coordinates for this model was chosen from the final values of QM/MM dynamics of the minimal model with anionic asp85. To retain a comparable computing time for the expanded model, part of the retinal was put into the MM region as depicted in Scheme 1b. With this partition, the initial coordinates of bacteriorhodopsin was energy minimized for 100 steps with GAMESS/CHARMM while treating the quantum mechanical atoms at the HF level using the 4-31G basis set and also a DFT calculation with the B3LYP functional using the same basis set. After energy minimization with each quantum method, QM/MM dynamic simulations were subsequently carried out with both HF and DFT methods using the same 4-31G basis set. Asp85 was treated as both an anion and protonated. At the level of B3LYP/4-31G for the quantum mechanical atoms with an anionic asp85, the average temperature and total energy for the last 500 steps of the 1 ps simulations were, respectively, 301.6 (2.5) K and −929217.3 (2.0) kcal/mol. These small fluctuations in both temperature and total energy indicate that the system has reached its equilibrium in subpicosecond range. Comparable conditions were reached for the protonated asp85 cases.

Results and Discussion

QM/MM Dynamic Simulations with Scheme 1a. The Schiff region of BR at the end of 4ps QM/MM dynamics simulations with HF/4-31G (Figure 1) displays two groups of four H-bonded waters in a hydrophobic channel comprising val49, leu93, and ala 210. One group consists of three water molecules H-bonded to the Schiff base nitrogen. The second group, which consists of the third and the fourth water molecules H-bonded to the carboxylate oxygen of asp96, overlaps the first group but is not aligned with it. The analysis of 4ps trajectory shows that the proton moved from the third water molecule to asp96 within

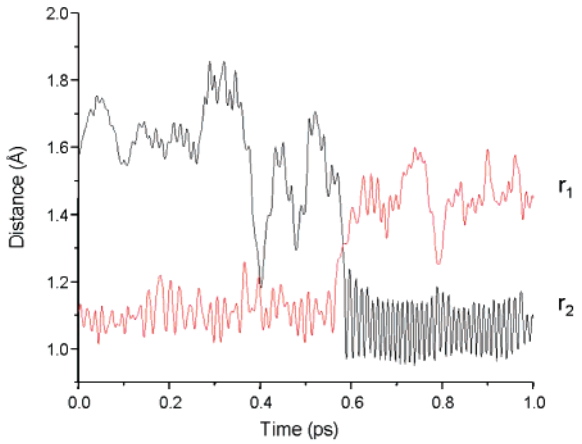

Figure 2. Proton transfer: r_1 is the distance between the asp96 carboxylate oxygen and its initially bound hydrogen, and r_2 is the distance between the Schiff base nitrogen and the hydrogen of the water molecule to which it is initially bound as depicted in Scheme 1b.

0.05 ps and then it took an additional 2 ps for water molecules to orient themselves to form a stable water chain as shown in Figure 1. No proton transfer, however, was seen from asp96 to the Schiff base nitrogen using the HF to represent the quantum region

Proton Transfer with Scheme 1b. The QM/MM region was expanded including asp85, thr89, and two additional water molecules into the QM region to better represent the proton-transfer environment in bacteriorhodopsin. In contrast to the lack of proton movement from asp96 with HF/4-31G for the QM region, complete proton transfer occurred from asp96 to the Schiff base nitrogen within 0.6 ps with the use of B3LYP/4-31G for the QM region and asp85 anionic. Proton transfer in the anionic asp85 case is described first because the process is calculated to be fastest and most direct for the cases considered here. The variation with time of the distance, r_1, of the asp96 carboxylate oxygen to its initially bound hydrogen in water 4, and r_2, the distance of the Schiff base nitrogen to the hydrogen of the neighboring water 1 to which it is initially bound, shows how the proton moves along the chain (Figure 2). For the first 0.5 ps, the distance r_1 and r_2 oscillates ranging from 1.1 to 1.3 Å and from 1.2 and 1.9 Å, respectively, without proton transfer. However, a short time after 0.55 ps the protons move from their initial bond, suggesting a concerted motion along the entire water chain. The snapshot at 0.5 ps (Figure 3a) shows that the hydrogen on the carboxylate oxygen of asp96 has not moved to the neighboring water molecule. However, short H-bonding distances ranging from 1.42 to 1.65 Å along the proton wire suggest that the initial partial proton transfer from asp96 introduces relatively strong ionic H-bonding interactions. The dynamical movement of the proton from the asp96 initiates ionic interactions that order the water molecules in the hydrophobic channel. Since the hydrophobic channel formed with val49, leu93, and ala210 does not have room for waters to cluster around the partially free proton, the ionic interactions project along the chain. At 0.582 ps (Figure 3b) the H-bonding distances along the chain are now short for all five H-bonds in the chain or the snapshot resembles the transition state for the proton wire. Both r_1 and r_2 in Figure 2 are now 1.31 Å, with the proton on the carboxylate oxygen of asp96 now shared with the neighboring water molecule, which in turn shares its proton with the third water molecule, forming a polarized hydronium ion with

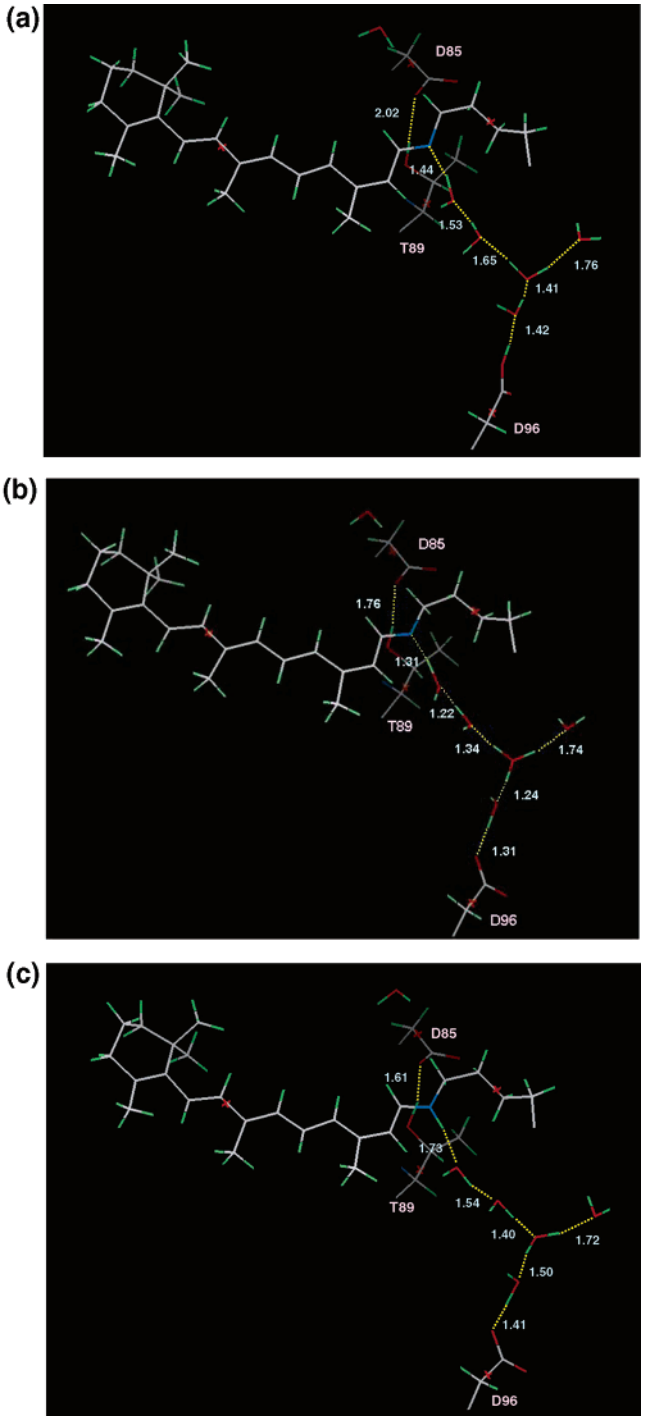

Figure 3. (a) Asp85 is anion. Snapshot at 0.5 ps while treating QM atoms at the level of B3LYP/4-31G. The proton on the carboxylate oxygen of asp96 has not moved to the neighboring water molecule. (b) Asp85 is anion. Snapshot at the transition state, 0.582 ps. The proton on the carboxylate oxygen of asp96 is shared with the neighboring water molecule, which in turn shares its proton with the neighboring water molecule forming a polarized hydronium ion. Overall H-bonding interactions have become even stronger as evidenced by short H-bond distances ranging from 1.22 to 1.34 Å. (c) Asp85 is anion. Snapshot at 0.65 ps. A full transfer of proton to the Schiff base nitrogen is seen. Asp96 is now negatively charged.

longer OH bonds than normal (Figure 3b). Overall H-bonding interactions have become even stronger as evidenced by short distances ranging from 1.22 to 1.34 Å or proton sharing. The formation of a very strong ionic H-bonded proton wire is likely to lower the energy barrier for proton translocation essentially

Table 1. Average Distances (Å) between Heavy Atoms from the 1 ps Trajectory at the Schiff Base Region[a]

	distances (Å)	
	anion	neutral
asp96OD2−O4	2.46 (0.05)	2.49 (0.06)
O4−O3	2.49 (0.07)	2.52 (0.08)
O3−O2	2.53 (0.10)	2.55 (0.07)
O2−O1	2.55 (0.08)	2.55 (0.06)
O1−N Schiff base	2.68 (0.12)	2.62 (0.12)

[a] Distances are defined in Scheme 1b. Parentheses indicate root-mean-square fluctuation

to zero. This provides a rationale for the observed sharp transition of distance r_1 and r_2 between 0.55 and 0.60 ps during which the proton transfer is essentially completed. Figure 3c illustrates a full transfer of hydrogen to the Schiff base nitrogen at 0.65 ps. There is still effective proton sharing that results in short heavy atom distances along the entire water chain as shown in Table 1. Waters found experimentally[34] in the region between asp96 and the Schiff base nitrogen are for a state of the photocycle that has relaxed from this fast proton-transfer event. However, waters 1 and 2 inserted in the hydrophobic region are observed in the X-ray structure for the final N state.

Thr89 maintains a strong ionic H-bond to the anionic asp85 through the transfer of the proton. The H-bonding distance between thr89 ands asp96 shortens from 2.02 to 1.61 Å as proton shuttles from asp96 to the Schiff base N. Once the proton has transferred there is an indication that asp85 is attracted somewhat toward the protonated Schiff base.

With neutral asp85, the OD1H group donates a proton to the OH group of thr89 while thr89 OH donates a proton to the backbone carbonyl of asp85. The proton on asp96 starts to propagate to a neighboring water molecule several times during a 2 ps interval but returns without completing the transfer. However, with the removal of water molecule 5 in Scheme 1b, the proton transfers to the Schiff base N in about 0.8 ps. Apparently, water molecule 5 which is branched out from the proton pathway hinders the proton transfer. With asp85 anionic, the proton gradient toward the Schiff base is large enough to overcome the hindrance of the proton transfer caused by water 5. Since the activation energy of the proton transfer with the DFT method is close to zero, small changes in the model or the basis set used in the calculation can have relatively large quantitative changes but not change the proton-transfer mechanism.

The state of protonation of the asp85 residue did not influence the formation of the proton wire ultimately, but there are still substantial oscillations in r_1 and r_2 as seen in Figure 4a before the completion of the transfer. The simulation was run to 2 ps with no indication that the proton returns to asp96. The final geometry of the QM region after the transfer with the protonated asp85 is shown Figure 4b. The distances between the heavy atoms that are involved in the proton transfer are given in Table 1 and are comparable to those obtained with the anionic asp85.

When the OH of thr89 is not H-bonded to the backbone carbonyl of neutral asp85, the proton from asp96 initially moves toward the neighboring water but the ionic interaction does not extend beyond this water. It is forestalled by the motion of the proton from asp85 transferring through thr89 and water 1 to

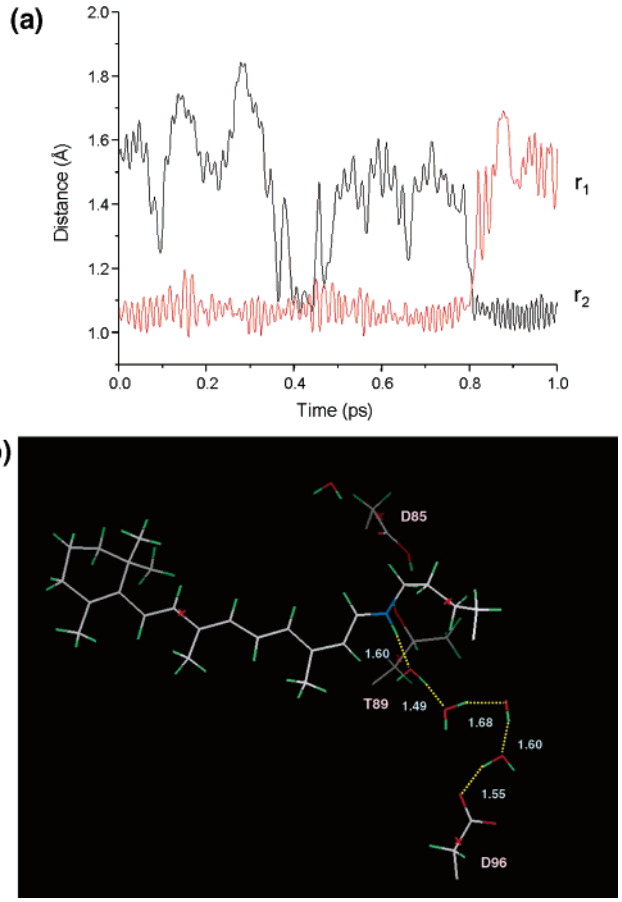

Figure 4. (a) Proton transfer: r_1 is the distance between the asp96 carboxylate oxygen and its initially bound hydrogen, and r_2 is the distance between the Schiff base nitrogen and the hydrogen of the water molecule to which it is initially bound. This is for the case with asp85 protonated. (b) Asp85 is protonated. Snapshot at 1.0 ps. The proton transfer to the Schiff base nitrogen is seen with asp96 negatively charged.

the Schiff base nitrogen irrespective of the presence of water 5. In this case, the fluctuation of the proton on asp85 now initiates proton transfer from thr89 to the Schiff base with concurrent transfer of the asp85 proton to thr89. Details of the back-transfer and movement of protein residues in the proton-transfer simulation with the neutral asp85 will be given later.

The hydrophobic channel primarily provides a repulsive wall with weak van der Waals interactions, allowing only a single chain of waters within the channel. The term hydrophobic channel has also been used in the description of other ion channels such as Gramicidin where it designates a mostly hydrophobic channel but there is either a single chain of backbone carbonyls or an occasional hydrophilic side-chain to which the waters can bind.[35] The rate-determining step in such a channel is the reordering of these dipoles after the passage of the charge. In the present case, the proton is not bound or impeded by any interaction of the same order as the ionic interactions within the proton wire.

Conclusion

The proton transfer from the carboxylate oxygen of asp96 to the Schiff base nitrogen is a very fast process, much less than a picosecond for the anionic asp85 and closer to 1 ps for the protonated asp85. Two waters are introduced into the hydro-

(34) Schobert, B.; Brown, L. S.; Lanyi, J. K. *J. Mol. Biol.* **2003**, *330*, 553−70.

(35) Roux, B. *Acc. Chem. Res.* **2002**, *35*, 366−75.

phobic part of the channel found in the M state structure[1] to complete the proton wire. They are dynamically ordered as the proton on asp96 interacts with and ultimately transfers to its neighboring water. The rate-limiting process in the proton transfer, therefore, must be developing the water channel and filling it with a single chain of water. Two waters are found in the recent X-ray structure of the N′ state[34] in the hydrophobic region near the Schiff base, thus validating our theoretical approach for adding waters in this region of the channel.

It is necessary to treat QM/MM atoms at the DFT/B3LYP level since the energy barrier for the proton transport process at the HF level is likely overestimated. With the DFT method no activation barrier is found for proton transfer. Changes in the model or the basis set will obviously vary the energy surface between the asp96 and the Schiff base so the barrier may appear although relatively small energy changes occur. In this step the dynamics of partial proton transfer from asp96 to a neighboring water molecule is a rate-determining step for the proton translocation. The ionic proton wire forms readily in a narrow hydrophobic cavity. Proton transfer occurs irrespective of the protonation state of asp85 if the H-bonding pattern for the protonated asp85 does not allow for back-transfer of the proton to the Schiff base in competition with the transfer from asp96. The dynamically protonated water chain orders itself through the strong ionic interactions. Transfer occurs with an effective barrier of the order of kT. Clustering by solvating the proton in a wider channel is likely to disrupt the formation of a 'proton wire' stretching the entire length of the channel involving five ionic strong H-bonds including four water molecules in both cases where the transfer occurs. After the formation of the water chain, proton transfer to the Schiff base nitrogen occurs within about 0.05 ps. The presence of water 5 has a larger effect on the protonated asp85 since the effective barrier for the proton transfer is raised by the loss of the attractive gradient from the anion. The organization of the water chain and the neighboring environment to stabilize the protonated Schiff base takes longer for the protonated asp85.

Acknowledgment. We are grateful to Dr. Bernard Brooks and Dr. Milan Hodoscek for letting us utilize the CHARMM/GAMESS software for this study. The use of Lobos Super computers at CIT/NIH is also gratefully acknowledged.

JA036115V